

# Study of magnetic iron nitride thin films deposited by high power impulse magnetron sputtering

Akhil Tayal<sup>1</sup>, Mukul Gupta<sup>1,\*</sup>, Ajay Gupta<sup>2</sup>, V. Ganesan<sup>1</sup>, Layanta Behera<sup>1</sup>, Surendra Singh<sup>3</sup>, and Saibal Basu<sup>3</sup>

<sup>1</sup>UGC-DAE Consortium for Scientific Research, University Campus, Khandwa Road, Indore-452 001, India

<sup>2</sup>Amity Center for Spintronic Materials, Amity University, Sector 125, Noida-201 303, India

<sup>3</sup>Solid State Physics Division, Bhabha Atomic Research Center, Mumbai-400 085, India

(Dated: November 25, 2014)

In this work, we studied phase formation, structural and magnetic properties of iron-nitride (Fe-N) thin films deposited using high power impulse magnetron sputtering (HiPIMS) and direct current magnetron sputtering (dc-MS). The nitrogen partial pressure during deposition was systematically varied both in HiPIMS and dc-MS. Resulting Fe-N films were characterized for their microstructure, magnetic properties and nitrogen concentration. We found that HiPIMS deposited Fe-N films show a globular nanocrystalline microstructure and improved soft magnetic properties. In addition, it was found that the nitrogen reactivity impedes in HiPIMS as compared to dc-MS. Obtained results can be understood in terms of distinct plasma properties of HiPIMS.

## I. INTRODUCTION

HiPIMS is a recently developed technique for the deposition of thin films. Unique plasma conditions associated with it, makes it a preferred choice over conventional deposition methods. [1–4] As compared to dc-MS, the plasma density in HiPIMS is of the order of  $10^{19}\text{m}^{-3}$ , about 2 orders of magnitude larger than that in dc-MS. [2] In HiPIMS plasma, number of ionized species exceeds neutrals. [2, 5] These characteristic properties of HiPIMS plasma results in improving film qualities such as film density, hardness, surface roughness, better adhesion, dense microstructure etc. Moreover, due to high metal ionization this technique has a better scope for controlling film properties deposited via reactive sputtering. As such HiPIMS has been frequently utilized for the deposition of metal nitrides such as Al-N, [6] Cr-N, [7–9] Ti-N, [10] Nb-N, [11] etc. and metal oxide thin films such as TiO<sub>2</sub>, [12, 13] Al<sub>2</sub>O<sub>3</sub>, [14, 15] ZnO, [16] ZrO<sub>2</sub>, [17] and Fe<sub>2</sub>O<sub>3</sub>. [18, 19] In these studies, it was observed that the properties of films deposited using reactive HiPIMS are superior. Konstantindis *et al.* found that formation of rutile phase in TiO<sub>2</sub> thin film is more favorable as compared to anatase phase when sputtered using HiPIMS. Moreover, HiPIMS deposited films show higher refractive index. [13] Ehasarian *et al.* observed that pretreatment using HiPIMS has improved the adhesion and mechanical properties of CrN thin films. [20] Similarly, Reinhard *et al.* observed improvement in corrosion resistance properties of HiPIMS treated CrN/NbN superlattice structure. [11] Recently, Zhao *et al.* observed that the optical transmittance of Zirconia thin films deposited using HiPIMS is more as compared to dc-MS. [17]

Looking at the vast capabilities of HiPIMS technique in depositing various kinds of thin films, it is surprising to note that HiPIMS processes have not yet been applied for the deposition of magnetic thin films with recent excep-

tion of Fe<sub>2</sub>O<sub>3</sub> [18, 19] and FeCuNbSiB. [21] Still magnetic nitride films have not yet been studied with HiPIMS. It is well known that transition metal magnetic nitrides are an important class of materials for their usage in various technological applications. [22, 23] Therefore, it will be immensely useful to study magnetic nitride films using HiPIMS.

It is well known that Fe-N compounds are interesting both from the basic and applied point of view. These compounds have a wide range of usage, such as in tribological coatings, magnetic read-write heads memory devices, etc. [24–26] In the present work we deposited a series of Fe-N films using HiPIMS and compared them with dc-MS. The structure (local and long range), growth and magnetic properties of the deposited thin films were investigated using various characterization techniques. We found that HiPIMS deposited Fe-N films show a globular nanocrystalline microstructure and improved soft magnetic properties. In addition, it was found that nitrogen reactivity impedes in HiPIMS as compared to dc-MS. The obtained results are presented and discussed in terms of plasma properties of HiPIMS.

## II. EXPERIMENTAL DETAILS

Fe-N thin films were deposited using HiPIMS and dc-MS techniques on Si(100) and float glass substrates using a AJA Int. Inc. make ATC Orion-8 series sputtering system. Pure Fe (purity 99.995%) target (diameter 75mm) was sputtered using a mixture of Ar and N<sub>2</sub> gases. Total gas flow was kept constant at 50 sccm and the relative partial pressure of nitrogen defined as  $R_{N_2} = P_{N_2} \times 100\% / [P_{N_2} + P_{Ar}]$ , (where  $P_{N_2}$  and  $P_{Ar}$  is nitrogen and argon gas flow) was kept at 0, 2, 5, 10, 20, 30, 40 and 50. Before deposition a base pressure of  $2 \times 10^{-6}$  Pa was achieved. During the deposition pressure was kept constant at 4 Pa using a dynamic throttling valve and substrate temperature was kept at 423 K. For HiPIMS, the deposition parameters used are: peak power 33.3 kW, peak voltage 700 V, peak current 47 A, pulse frequency

\* mgupta@csr.res.in/dr.mukul.gupta@gmail.com

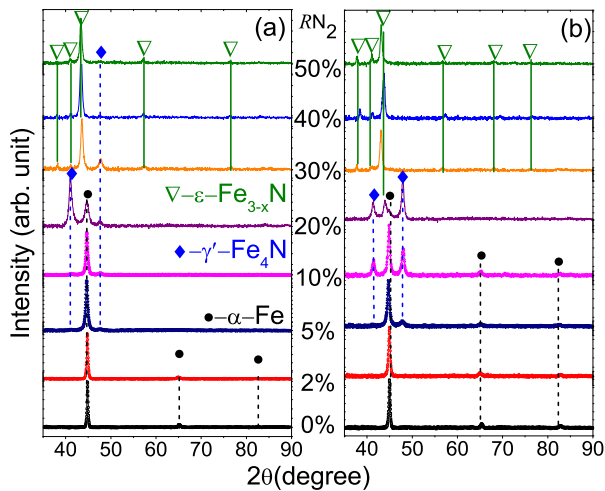


FIG. 1. (Color online) X-ray diffraction patterns of Fe-N thin films prepared at varying  $R_{N_2}$  using HiPIMS(a) and dc-MS(b) techniques.

60 Hz, pulse duration  $150 \mu\text{s}$  and average power 300 W. For dc-MS sputtering power was kept at 100 W. Typical thickness of deposited films was kept about 80-100 nm.

Structural characterizations of the samples were carried out with x-ray diffraction (XRD) using a standard x-ray diffractometer (Bruker D8 Advance) equipped with  $\text{Cu K}\alpha$  x-rays source in  $\theta - 2\theta$  geometry. Surface morphology was obtained using atomic force microscopy (AFM) using a Digital Instruments make Nanoscope E AFM system with a  $\text{Si}_3\text{N}_4$  cantilever. Magnetic properties were studied using a Quantum Design make superconducting quantum interference device-vibrating sample magnetometer (S-VSM) and polarized neutron reflectivity (PNR). PNR measurements were performed at Dhruva Reactor of Bhaba Atomic Research Center, Mumbai. [27] A magnetic field of strength 2000 Oe was applied along the films plane to saturate samples magnetically. The local structure of nitrogen was studied using soft x-ray absorption spectroscopy (SXAS) at BL-1 beamline of Indus-2 synchrotron radiation source at RRCAT, Indore. [28] SXAS measurements were performed in an UHV chamber in total electron yield (TEY) mode. For accurate measurements of nitrogen concentration,  $^{14}\text{N}$  depth profiles were measured using secondary ion mass spectroscopy (SIMS) technique (Hiden Analytical SIMS Workstation). For sputtering  $\text{O}_2^+$  primary ions were used with 5 keV energy and 400 nA beam current. SIMS measurements were performed in an UHV chamber with a base pressure of the order of  $8 \times 10^{-8}$  Pa, during measurements the chamber pressure was  $8 \times 10^{-6}$  Pa.

### III. RESULTS AND DISCUSSION

Phase formation of Fe-N thin films has been extensively studied by several co-workers using different thin film deposition techniques such as magnetron sputtering, [29, 30] ion beam sputtering, [31, 32] e-beam evaporation, [33] pulsed laser deposition, [34, 35] etc. In general,

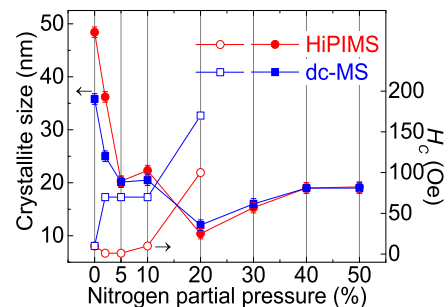


FIG. 2. (Color online) Variation of crystallite size and coercivity with increasing nitrogen partial pressure. Here solid and open symbols represent crystallite size and coercivity, respectively for HiPIMS and dc-MS samples.

as nitrogen partial pressure is increased in a physical vapor deposition method, different types of Fe-N phases are formed and they can be broadly classified as: nanocrystalline  $\alpha\text{-Fe-N} \rightarrow$  amorphous  $\alpha\text{-Fe-N} \rightarrow \alpha''\text{-Fe}_{16}\text{N}_2 \rightarrow \gamma'\text{-Fe}_4\text{N} \rightarrow \varepsilon\text{-Fe}_{3-z}\text{N} (0 \leq z \leq 1) \rightarrow \zeta\text{-Fe}_2\text{N} \rightarrow \gamma'''\text{-FeN} \rightarrow$  amorphous/nanocrystalline  $\gamma'''\text{-FeN}$ . Since formation of Fe-N phases with HiPIMS has not yet been studied, we deposited a series of Fe-N samples using HiPIMS and compared them with its sibling i.e. dc-MS.

Figure 1 shows XRD patterns of Fe-N thin films deposited using HiPIMS(a) and dc-MS(b) at different nitrogen partial pressures. For  $R_{N_2}=0$  and 2%, the structure is  $bcc$   $\alpha\text{-Fe}$ , both with HiPIMS and dc-MS. As  $R_{N_2}$  increases,  $\alpha\text{-Fe}$  structure is predominantly preserved up to  $R_{N_2} = 10\%$  in HiPIMS with faint peaks corresponding to  $\gamma'$ , whereas for dc-MS samples the amount of  $\gamma'$  phase appears to be larger. At  $R_{N_2}=20\%$ , intensity of peaks corresponding to  $\gamma'$  phase increases in HiPIMS but in dc-MS samples along with  $\alpha\text{-Fe(N)}$  and  $\gamma'$  phases, peak corresponding to  $\varepsilon$  phase can also be seen. Further increase in  $R_{N_2}$  from 30% to 50% leads to formation of  $\varepsilon$  phase in both cases, but faint peaks corresponding to  $\gamma'$  can only be seen even up to  $R_{N_2}=50\%$  in HiPIMS samples. Observed phase formation with varying  $R_{N_2}$  is similar in dc-MS to that observed in the literature, but appears to be somewhat different for HiPIMS deposited samples.

To see the variation of crystallite size with increasing  $R_{N_2}$ , average crystallite size ( $d$ ) was calculated using Scherrer formula (for the most intense peak):  $d = 0.9\lambda/b \cos \theta$  [36], and shown in figure 2 [with  $\lambda$  wavelength of x-rays,  $b$  an angular width in terms of  $2\theta$  and  $\theta$  is Bragg angle]. As such crystallite sizes are similar in both cases except for  $R_{N_2}=0$  and 2%, where HiPIMS samples have significantly larger crystallite sizes as compared with dc-MS.

We did S-VSM and PNR measurements on selected samples to measure the coercivity ( $H_C$ ) and the saturation magnetization ( $M_S$ ), respectively. Figure 3 shows normalized magnetization with applied magnetic field (M-H) loops of Fe-N samples deposited by varying the  $R_{N_2}$  using HiPIMS[(a1)-(e1)] and dc-MS[(a2)-(e2)] tech-

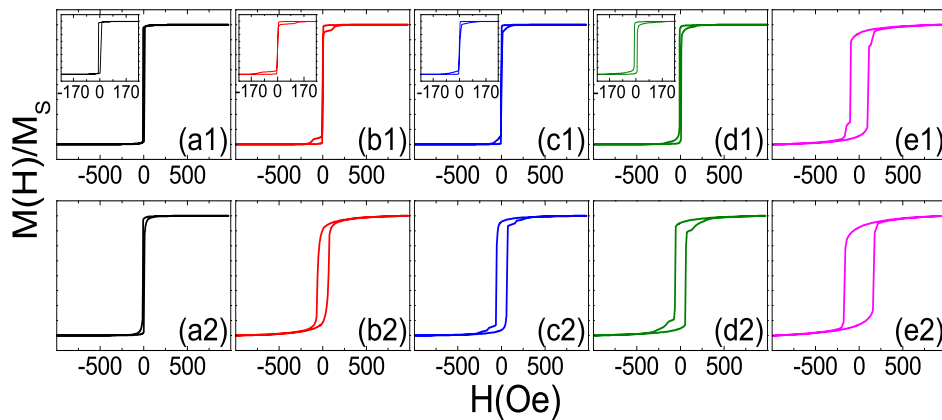


FIG. 3. (Color online) Normalized M-H loops of Fe-N thin films deposited using HiPIMS[(a1)-(e1)] and dc-MS[(a2)-(e2)] at  $R_{N_2}=0\%$ [(a1),(a2)],  $2\%$ [(b1),(b2)],  $5\%$ [(c1),(c2)],  $10\%$ [(d1),(d2)], and  $20\%$ [(e1),(e2)]. Inset of figure[(a1)-(d1)] shows blown up region of M-H loops near the coercive field.

niques. It can be seen that the M-H loops of pure Fe films are almost identical both for HiPIMS and dc-MS, with  $H_C \sim 10$  Oe. As nitrogen is introduced during the deposition,  $H_C$  increases suddenly to a value of about 70 Oe, for dc-MS samples and remains at this value up to  $R_{N_2}=10\%$ . However, this behavior is strikingly different for HiPIMS samples; while  $H_C$  appears to be negligible for  $R_{N_2} = 2$  and  $5\%$  [inset of figure 3[(a1)-(d1)]] samples, it increases to about 10 Oe for  $R_{N_2}=10\%$ . At  $R_{N_2}=20\%$ ,  $H_C$  increases in both samples, its value is about 100 Oe and 170 Oe for HiPIMS and dc-MS samples, respectively. Typical error bars in measuring  $H_C$  are about  $\pm 5$  Oe.

The observed variation in the  $H_C$  may stem either due to particle size effect [explained by random anisotropy model (RAM) [37, 38]] or stresses present in the samples. According to RAM, when particle size is above the ferromagnetic exchange length ( $L_{ex}$ ), the  $H_C$  increases with decreasing the particle size, and for the particle size below  $L_{ex}$ , the  $H_C$  decreases with decreasing the particle size. Generally, the value of  $L_{ex} \sim 30$  nm, for pure iron [29, 39] and expected to vary only slightly for iron nitride thin films. [40] In the present case observed variation in the  $H_C$  does not correlate with the change in the crystallite size with increasing  $R_{N_2}$  [see figure 2]. It indicates that the observed variance in the  $H_C$  can not be explained in terms of RAM. Therefore, it is expected that the other phenomenon may be dominant here.

It is known that HiPIMS plasma is highly ionized as compared to dc-MS even though the energies of adatoms are only slightly higher in HiPIMS ( $\sim 20$  eV). Such conditions lead to denser films with the relatively smaller amount of defects and vacancies in HiPIMS as compared to dc-MS. [2, 4, 41] Relatively smaller density of defects could result in smaller stress in the deposited films. This effect lead to improve soft-magnetic properties of films deposited using HiPIMS. The sudden increase in  $H_C$  for  $R_{N_2} = 20\%$ , can be understood in terms of change in the crystal structure as discussed in our XRD results. It may be noted that M-H loops of HiPIMS samples are

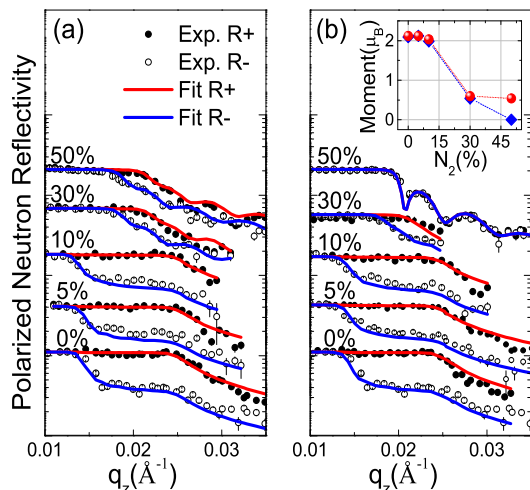


FIG. 4. (Color online) PNR patterns of Fe-N thin films prepared using HiPIMS(a) and dc-MS(b) at varying nitrogen partial pressure. Inset of figure(b) shows variation of average magnetic moment with increasing nitrogen partial pressure.

somewhat asymmetric, which could be due to growth of  $\gamma'$  along with  $\alpha$ -Fe phase, also inferred with XRD data.

To investigate the variation in average magnetic moment with increasing nitrogen partial pressure, PNR measurements were performed. It is known that PNR is a very precise tool to measure accurate average magnetic moment specially for magnetic thin films, as it is insensitive to thin film dimensions. [42] Figure 4 shows PNR patterns of Fe-N thin films deposited using HiPIMS(a) and dc-MS(b) prepared at varying  $R_{N_2}$ . The obtained PNR patterns were fitted using a computer program based on the Parratt formalism [43] and the average magnetic moment was calculated. Inset of figure 4(b) shows the variation of magnetic moment with increasing  $R_{N_2}$ . It can be seen that up to  $R_{N_2}=10\%$ , magnetic moment of the samples does not show any variation (within experimen-

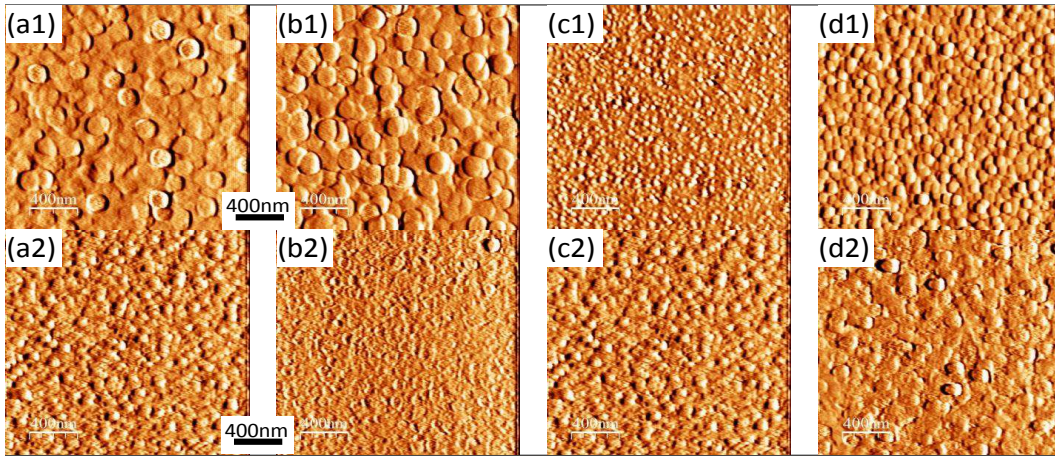


FIG. 5. (Color online) AFM images of Fe-N thin films prepared using HiPIMS[(a1)-(d1)] and dc-MS[(a2)-(d2)] at  $R_{N_2} = 0\%$ [(a1),(a2)],  $2\%$ [(b1),(b2)],  $5\%$ [(c1),(c2)], and  $10\%$ [(d1),(d2)].

tal accuracy) both for dc-MS and HiPIMS. However, at  $R_{N_2} = 20\%$  there is a sudden decrease in the value of magnetic moment in both the cases. Interestingly, the sample deposited using dc-MS at  $R_{N_2} = 50\%$  becomes non-magnetic, whereas, it remains magnetic at this nitrogen partial pressure when deposited using HiPIMS. It is known that the formation of non-magnetic iron nitrides with increasing nitrogen concentration is only observed when N concentration  $> 30\text{at.}\%$ . [34, 44] As non-magnetic Fe-N phase is only observed in case of films prepared using dc-MS, it indicates that nitrogen incorporation has increased in the samples prepared using dc-MS as compared to HiPIMS.

The surface morphology of samples was investigated using AFM and shown in figure 5 for HiPIMS[(a1)-(d1)] and dc-MS[(a2)-(d2)] at  $R_{N_2} = 0\%$ [(a1),(a2)],  $2\%$ [(b1),(b2)],  $5\%$ [(c1),(c2)], and  $10\%$ [(d1),(d2)]. The scan area for all measurements was kept constant at  $2\mu\text{m} \times 2\mu\text{m}$ . For HiPIMS samples, the AFM images indicate that the particle size distribution is more uniform than that in dc-MS. Recently it was observed that in HiPIMS deposited films, due to high ionized flux and moderate adatoms energy, surface mobility increases. This process results in repeated nucleation process, [4] resulting in a transition from columnar growth (as in dc-MS) to formation of globular nanocrystalline microstructure as observed in the present case. [41, 45]

Soft x-ray absorption spectroscopy is a tool to investigate the local structure of nitrogen atoms. We did SXAS measurements near nitrogen K-edge. Obtained spectrum are shown in figure 6 for selected samples deposited at  $R_{N_2} = 5\%$ ,  $20\%$ , and  $50\%$  using HiPIMS(a) and dc-MS(b). Generally, a SXAS spectrum of metal nitrides consists of five features as observed in our samples. These features are assigned as (i) I-transition from  $N 1s$  to the unoccupied hybridized state of  $Fe 3d - t_{2g}$  and  $N 2p$  (ii) II-transition from  $N 1s$  to hybridized  $Fe 3d - e_g$  and  $N 2p$  state (iii) III, IV, V- transition from

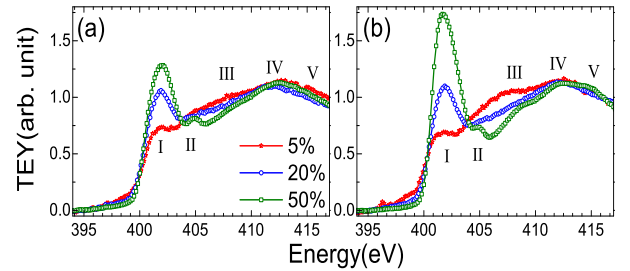


FIG. 6. (Color online) Nitrogen K-edge x-ray absorption spectrum of iron nitride thin films prepared using HiPIMS(a) and dc-MS(b) at varying  $R_{N_2}$ .

$N 1s$  to hybridized  $N 2p$  and  $Fe 4sp$  state. [46–49] In order to compare the relative nitrogen concentration for HiPIMS and dc-MS samples, background before pre-edge and after post-edge was subtracted using a computer program IFEFFIT-Athena. [50] As can be seen from figure 6 that the intensity of feature I increases with increasing  $R_{N_2}$  both for HiPIMS and dc-MS samples. However, the relative intensity of feature I (for  $R_{N_2} = 50\%$ ), is significantly enhanced in dc-MS deposited sample as compared to that in HiPIMS sample. Since the edge intensity in the XAS pattern is proportional to the nitrogen concentration, [51] the obtained results clearly indicate that nitrogen concentration is higher for the samples prepared using dc-MS as compared to HiPIMS.

From the above analysis using various characterization techniques it appears that the amount of nitrogen in HiPIMS deposited samples is less than that in dc-MS. In order to quantify N concentration, we did SIMS measurements. From SIMS depth profiles, atomic concentration of a element  $A$  in the matrix of element  $B$ , can be calculated using a following expression:

$$C_A = R S F_A \times \frac{I_A}{I_B} \quad (1)$$

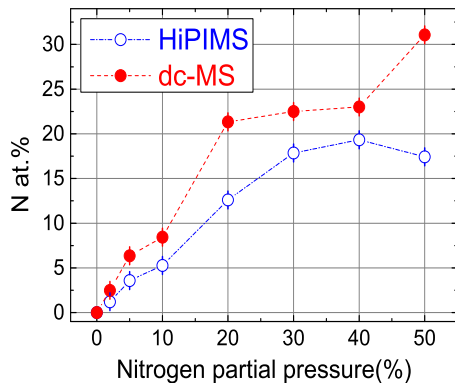


FIG. 7. (Color online) Variation of atomic concentration of nitrogen with increasing nitrogen partial pressure deposited using HiPIMS and dc-MS techniques.

Where,  $C_A$  is atomic concentration,  $RSF_A$  is relative sensitive factor and  $I_A$  or  $I_B$  is observed intensity in a SIMS depth profile for element  $A$  or  $B$ . In general, exact calculation of  $RSF$  is a tedious process due to involved matrix effects, but in the simplest case of two elements  $RSF$  can be calculated by using a reference sample with known concentration.[23, 52] Using equation 1 we measured N at.% both for HiPIMS and dc-MS samples. Figure 7 shows the observed variation of nitrogen concentration with increasing  $R_{N_2}$ . It can be seen that up to  $R_{N_2}=20\%$ , N at.% increases almost linearly in both cases. Between  $R_{N_2}$  20 to 40%, N at.% increases marginally but there is a sudden jump at  $R_{N_2}=50\%$  in dc-MS. In contrast, a linear increase in N at.% can be seen almost up to  $R_{N_2}=40\%$ , and get saturated for  $R_{N_2}=50\%$  in HiPIMS. However, overall N at.% is always higher in dc-MS as compared to HiPIMS.

Intuitively, it may appear that the nitrogen concentration should be more for HiPIMS deposited samples as compared to dc-MS due to highly ionized flux in HiPIMS. However, as observed in other nitride systems

such as CrN, [53, 54] TiN, [53, 55] TiO<sub>2</sub>, [56, 57] etc. the amount of reactive gas get reduced in HiPIMS because of significantly higher temperature produced in HiPIMS due to high power impulse (33.3 kW for 150  $\mu$ s). This leads to expansion of reactive gas in the vicinity of a target, reducing the volume of available gas for reaction. This phenomenon is generally known as ‘gas-rarefaction’. [2, 4, 56, 57]

#### IV. CONCLUSION

The results obtained from this work provide some distinct properties of Fe-N films deposited using HiPIMS as compared to dc-MS deposited films (i) soft magnetic properties Fe-N films improve (ii) N incorporation in Fe impedes (iii) the microstructure is globular type rather than columnar. Highly ionized flux and moderate ion energy in the HiPIMS plasma results in high adatom mobility leading to the observed effects. A reduction in N concentration in HiPIMS deposited films as compared to dc-MS for a similar value of  $R_{N_2}$  can be understood by ‘gas-rarefaction’ phenomenon caused by substantially high temperatures in HiPIMS process.

#### ACKNOWLEDGMENTS

We acknowledge D. M. Phase, D. K. Shukla, R. Sah and S. Karwal for utilization of SXAS beamline. Help provided in AFM measurements by M. Gangrade, and in S-VSM measurements by R. J. Choudhary and P. Pandey is gratefully acknowledged. One of the author (A. T.) wants to acknowledge CSIR, New Delhi for a research fellowship.

#### REFERENCES

- [1] J. Andersson and A. Anders, Phys. Rev. Lett. **102**, 045003 (Jan 2009), <http://link.aps.org/doi/10.1103/PhysRevLett.102.045003>
- [2] J. T. Gudmundsson, N. Brenning, D. Lundin, and U. Helmersson, Journal of Vacuum Science and Technology A **30**, 030801 (2012), <http://scitation.aip.org/content/avs/journal/jvsta/30/3/10.1116/1.3691832>
- [3] A. Anders, J. Andersson, and A. Ehasarian, Journal of Applied Physics **102**, 113303 (2007), <http://scitation.aip.org/content/aip/journal/jap/102/11/10.1063/1.2817812>
- [4] D. Lundin and K. Sarakinos, Journal of Materials Research **27**, 780 (3 2012), ISSN 2044-5326
- [5] K. Sarakinos, J. Alami, and S. Konstantinidis, Surface and Coatings Technology **204**, 1661 (2010), ISSN 0257-8972, <http://www.sciencedirect.com/science/article/pii/S0257897209009426>
- [6] A. Guillaumot, F. Lapostolle, C. Dublanche-Tixier, J. Oliveira, A. Billard, and C. Langlade, Vacuum **85**, 120 (2010), ISSN 0042-207X, <http://www.sciencedirect.com/science/article/pii/S0042207X10001612>
- [7] A. P. Ehasarian, J. G. Wen, and I. Petrov, Journal of Applied Physics **101**, 054301 (2007), <http://scitation.aip.org/content/aip/journal/jap/101/5/10.1063/1.2697052>
- [8] J. Lin, W. D. Sproul, J. J. Moore, S. Lee, and S. Myers, Surface and Coatings Technology **205**, 3226 (2011), ISSN 0257-8972, <http://www.sciencedirect.com/science/article/pii/S0257897210012132>
- [9] M. Hala, N. Viau, O. Zabeida, J. E. Klemberg-Sapieha, and L. Martinu, Journal of Applied Physics **107**, 043305 (2010), <http://scitation.aip.org/content/>

- aip/journal/jap/107/4/10.1063/1.3305319
- [10] M. Lattemann, U. Helmersson, and J. Greene, *Thin Solid Films* **518**, 5978 (2010), ISSN 0040-6090, <http://www.sciencedirect.com/science/article/pii/S0040609010007340>
- [11] C. Reinhard, A. Ehasarian, and P. Hovsepian, *Thin Solid Films* **515**, 3685 (2007), ISSN 0040-6090, <http://www.sciencedirect.com/science/article/pii/S0040609006013332>
- [12] M. Aiempnanakit, U. Helmersson, A. Aijaz, P. Larsson, R. Magnusson, J. Jensen, and T. Kubart, *Surface and Coatings Technology* **205**, 4828 (2011), ISSN 0257-8972, <http://www.sciencedirect.com/science/article/pii/S0257897211004270>
- [13] S. Konstantinidis, J. Dauchot, and M. Hecq, *Thin Solid Films* **515**, 1182 (2006), ISSN 0040-6090, proceedings of the 33rd International Conference on Metallurgical Coatings and Thin Films {ICMCTF} 2006, <http://www.sciencedirect.com/science/article/pii/S0040609006009060>
- [14] E. Wallin and U. Helmersson, *Thin Solid Films* **516**, 6398 (2008), ISSN 0040-6090, <http://www.sciencedirect.com/science/article/pii/S0040609007015374>
- [15] E. Wallin, T. I. Selinder, M. Elfving, and U. Helmersson, *EPL (Europhysics Letters)* **82**, 36002 (2008), <http://stacks.iop.org/0295-5075/82/i=3/a=36002>
- [16] S. Konstantinidis, A. Hemberg, J. P. Dauchot, and M. Hecq, *Journal of Vacuum Science and Technology B* **25** (2007)
- [17] X. Zhao, J. Jin, J.-C. Cheng, J.-W. Lee, K.-H. Wu, K.-C. Lin, J.-R. Tsai, and K.-C. Liu, *Thin Solid Films*, (2014), ISSN 0040-6090, <http://www.sciencedirect.com/science/article/pii/S004060901400635X>
- [18] S. Kment, Z. Hubicka, J. Krysa, J. Olejnick, M. Cada, I. Gregora, M. Zlamal, M. Brunclikova, Z. Remes, N. Liu, L. Wang, R. Kirchgeorg, C. Lee, and P. Schmuiki, *Catalysis Today* **230**, 8 (2014), ISSN 0920-5861, selected contributions of the 4th International Conference on Semiconductor Photochemistry (SP4), <http://www.sciencedirect.com/science/article/pii/S0920586113006500>
- [19] Z. Hubika, S. Kment, J. Olejnek, M. Cada, T. Kubart, M. Brunclikova, P. Krov, P. Admek, and Z. Reme, *Thin Solid Films* **549**, 184 (2013), ISSN 0040-6090, the 40th International Conference on Metallurgical Coatings and Thin Films, <http://www.sciencedirect.com/science/article/pii/S0040609013014995>
- [20] A. Ehasarian, P. Hovsepian, L. Hultman, and U. Helmersson, *Thin Solid Films* **457**, 270 (2004), ISSN 0040-6090, <http://www.sciencedirect.com/science/article/pii/S0040609003017115>
- [21] I.-L. Velicu, M. Neagu, H. Chiriac, V. Tiron, and M. Dobromir, *Magnetics, IEEE Transactions on* **48**, 1336 (April 2012), ISSN 0018-9464
- [22] J. M. D. Coey and P. A. I. Smith, *J. Magn. Magn. Mat.* **200**, 405 (1999)
- [23] A. Tayal, M. Gupta, N. P. Lalla, A. Gupta, M. Horisberger, J. Stahn, K. Schlage, and H.-C. Wille, *Phys. Rev. B* **90**, 144412 (Oct 2014), <http://link.aps.org/doi/10.1103/PhysRevB.90.144412>
- [24] C. Navío, J. Alvarez, M. J. Capitan, F. Yndurain, and R. Miranda, *Phys. Rev. B* **78**, 155417 (2008)
- [25] C. Navío, J. Alvarez, M. J. Capitan, J. Camarero, and R. Miranda, *Appl. Phys. Lett.* **94**, 263112 (2009)
- [26] Y.-K. Liu and M. H. Kryder, *Appl. Phys. Lett.* **77**, 426 (2000), <http://dx.doi.org/doi/10.1063/1.126998>
- [27] S. Basu and S. Singh, *Journal of Neutron Research* **14**, 109 (2006), <http://www.tandfonline.com/doi/pdf/10.1080/10238160500475301>, <http://www.tandfonline.com/doi/abs/10.1080/10238160500475301>
- [28] D. M. Phase, M. Gupta, S. Potdar, L. Behera, R. Sah, and A. Gupta, *AIP Conference Proceedings* **1591**, 685 (2014), <http://scitation.aip.org/content/aip/proceeding/aipcp/10.1063/1.4872719>
- [29] R. Gupta and M. Gupta, *Phys. Rev. B* **72**, 024202 (2005)
- [30] E. B. Easton, T. Buhrmester, and J. Dahn, *Thin Solid Films* **493**, 60 (2005), ISSN 0040-6090, <http://www.sciencedirect.com/science/article/pii/S0040609005007030>
- [31] D. M. Borsa and D. O. Boerma, *Hyp.Int.* **151-152**, 31 (2003)
- [32] X. Zhao Ding, F. Min Zhang, J. Sheng Yan, H. Lie Shen, X. Wang, X. Huai Liu, and D.-F. Shen, *J. Appl. Phys.* **82**, 5154 (1997)
- [33] M. Vergnat, P. Bauer, H. Chatbi, and G. Marchal, *Thin Solid Films* **275**, 251 (1996), ISSN 0040-6090, <http://www.sciencedirect.com/science/article/pii/S0040609095070559>
- [34] P. Schaaf, *Prog. Mater. Sci.* **47**, 1 (2002)
- [35] M. Gupta, A. Gupta, P. Bhattacharya, P. Misra, and L. Kukreja, *J. Alloys and Compounds* **326**, 265 (2001), ISSN 0925-8388, <http://www.sciencedirect.com/science/article/pii/S0925838801013160>
- [36] B. D. Cullity, *Elements of X-ray Diffraction* (Addison-Wesley, MA, 1978)
- [37] G. Herzer, *I.E.E.E. Trans. Mag.* **25**, 3327 (1989)
- [38] J. F. Löffler, H.-B. Braun, and W. Wagner, *Phys. Rev. Lett.* **85**, 1990 (Aug 2000), <http://link.aps.org/doi/10.1103/PhysRevLett.85.1990>
- [39] J. F. Löffler, J. P. Meier, B. Doudin, J.-P. Ansermet, and W. Wagner, *Phys. Rev. B* **57**, 2915 (1998)
- [40] X. Bao, R. M. Metzger, and W. D. Doyle, *Journal of Applied Physics* **73** (1993)
- [41] E. Lecoq, J. Guillot, D. Duday, J.-B. Chemin, and P. Choquet, *Journal of Physics D: Applied Physics* **47**, 195201 (2014), <http://stacks.iop.org/0022-3727/47/i=19/a=195201>
- [42] S. J. Blundell and J. A. C. Bland, *Phys. Rev. B* **46**, 3391 (Aug 1992), <http://link.aps.org/doi/10.1103/PhysRevB.46.3391>
- [43] L. G. Parratt, *Phys. Rev.* **95**, 359 (1954)
- [44] G. Chen, N. Jaggi, J. Butt, E. Yeh, and L. Schwartz, *Journal of physical chemistry* **87**, 5326 (1983)
- [45] J. Alami, K. Sarakinos, F. Uslu, and M. Wuttig, *Journal of Physics D: Applied Physics* **42**, 015304 (2009), <http://stacks.iop.org/0022-3727/42/i=1/a=015304>
- [46] J. Pflugger, J. Fink, G. Crecelius, K. Bohnen, and H. Winter, *Solid State Communications* **44**, 489 (1982), ISSN 0038-1098, <http://www.sciencedirect.com/science/article/pii/0038109882901302>
- [47] F. Esaka, H. Shimada, M. Imamura, N. Matsubayashi, T. Sato, A. Nishijima, A. Kawana,

- H. Ichimura, T. Kikuchi, and K. Furuya, *Thin Solid Films* **281282**, 314 (1996), ISSN 0040-6090, <http://www.sciencedirect.com/science/article/pii/S0040609096886408>
- [48] C. Mitterbauer, C. HAbert, G. Kothleitner, F. Hofer, P. Schattschneider, and H. Zandbergen, *Solid State Communications* **130**, 209 (2004), ISSN 0038-1098, <http://www.sciencedirect.com/science/article/pii/S0038109804000936>
- [49] I. Jouanny, P. Weisbecker, V. Demange, M. Grafouté, O. Peña, and E. Bauer-Grosse, *Thin Solid Films* **518**, 1883 (2010)
- [50] B. Ravel and M. Newville, *Journal of Synchrotron Radiation* **12**, 537 (Jul 2005), <http://dx.doi.org/10.1107/S0909049505012719>
- [51] Y. Kihn, C. Mirguet, and L. Calmels, *Journal of Electron Spectroscopy and Related Phenomena* **143**, 117 (2005), ISSN 0368-2048, electron Energy Loss Spectroscopy in the Electron Microscope Electron Energy Loss Spectroscopy in the Electron Microscope, <http://www.sciencedirect.com/science/article/pii/S0368204804004098>
- [52] M. Py, J. P. Barnes, D. Lafond, and J. M. Hartmann, *Rapid Communications in Mass Spectrometry* **25**, 629 (2011), ISSN 1097-0231, <http://dx.doi.org/10.1002/rcm.4904>
- [53] A. Vetushka and A. P. Ehiasarian, *Journal of Physics D: Applied Physics* **41**, 015204 (2008), <http://stacks.iop.org/0022-3727/41/i=1/a=015204>
- [54] G. Greczynski and L. Hultman, *Vacuum* **84**, 1159 (2010), ISSN 0042-207X, <http://www.sciencedirect.com/science/article/pii/S0042207X10000795>
- [55] F. Mitschker, M. Prenzel, J. Benedikt, C. Maszl, and A. von Keudell, *Journal of Physics D: Applied Physics* **46**, 495201 (2013), <http://stacks.iop.org/0022-3727/46/i=49/a=495201>
- [56] K. Sarakinos, J. Alami, and M. Wuttig, *Journal of Physics D: Applied Physics* **40**, 2108 (2007), <http://stacks.iop.org/0022-3727/40/i=7/a=037>
- [57] C. Huo, M. A. Raadu, D. Lundin, J. T. Gudmundsson, A. Anders, and N. Brenning, *Plasma Sources Science and Technology* **21**, 045004 (2012), <http://stacks.iop.org/0963-0252/21/i=4/a=045004>